Ann Mov Disord. Author manuscript; available in PMC 2022 August 05.

Published in final edited form as:
Ann Mov Disord. 2021 May 31; 4(2): 60–65. doi:10.4103/AOMD.AOMD_41_20.

Morphometric mapping of the macrostructural abnormalities of midsagittal corpus callosum in Wilson's disease

Albert Stezin,

Venkateswara Reddy Reddam[1], **Shantala Hegde**[2], **Ravi Yadav**[1], **Jitender Saini**[3], **Dr. Pramod Kumar Pal**[1]

[1]Department of Clinical Neuroscience and Department of Neurology, Department of Neurology, National Institute of Mental Health and Neurosciences, Bangalore, Karnataka, India

[2]Department of Neuropsychology, National Institute of Mental Health and Neurosciences, Bangalore, Karnataka, India

[3]Department of Neuroimaging and Interventional Radiology, National Institute of Mental Health and Neurosciences, Bangalore, Karnataka, India

Abstract

Background and Purpose—The corpus callosum (CC) consists of topographically arranged white matter (WM) fibers. Previous studies have indicated the CC to be discretely involved in WD. In this study, we strived to characterize the macrostructural properties of the CC using midsagittal cross-sectional area and thickness profile measurements.

Materials and Methods—This study was performed using archived magnetic resonance imaging (MRI) scans of 14 patients with WD and 14 age- and gender-matched healthy controls. Using an automated software pipeline for morphometric profiling, the midsagittal CC was segmented into five sub-regions ($CC_{1–5}$) according to the Hofer–Frahm scheme. The mean thickness and area of different CC segments and their clinical and cognitive correlates were identified.

Results—The mean area was significantly different only in CC_2 segment (94.2 ± 25.5 vs. 118.6 ± 19.7 mm^2, corrected $P < 0.05$). The mean thickness was significantly different in CC_1 (5.06 ± 1.15 vs. 6.93 ± 0.89 mm, corrected $P < 0.05$), CC_2 (3.73 ± 0.96 vs. 4.87 ± 1.01 mm, corrected $P < 0.05$), and CC_3 segments (3.42 ± 0.84 vs. 3.94 ± 0.72 mm, corrected $P < 0.05$). The age at onset of neurological symptoms and MMSE score was significantly correlated with the morphometric changes of CC_1 and CC_2 segments.

Correspondence to: Pramod Kumar Pal.

Address for correspondence: Dr. Pramod Kumar Pal, Department of Neurology, National Institute of Mental Health and Neurosciences (NIMHANS), Hosur Road, Bangalore 560029, Karnataka, India. palpramod@hotmail.com.

Conflicts of interest
There are no conflicts of interest.

Europe PMC Funders Author Manuscripts

Conclusion—Morphological changes of the CC are discrete in WD. Morphometric loss of CC was associated with an earlier onset of neurological symptoms and cognitive dysfunction in WD.

Keywords

Cognitive dysfunction; corpus callosum; magnetic resonance imaging; MMSE; white matter; Wilson disease

Introduction

The corpus callosum (CC) is comprised of 250–300 million axons and is the largest inter-hemispheric white matter (WM) tract of the brain.[1,2] It connects different homologous areas on either side of the brain.[3–5] The number of CC fibers are believed to be fixed from birth and the morphological changes across lifespan usually result from myelination, degeneration, and pruning changes.[6]

Although the CC does not have anatomical subregions, dissection and neuroimaging studies have proposed different functional parcellation schemes to subdivide the CC.[7,8] These parcellation techniques have recently been utilized to study the morphometric changes of CC in different diseases. In particular, a decrease in the thickness and area of CC segments with significant correlation with cognitive dysfunction is known in psychosis, Parkinson's disease, and Alzheimer's disease.[9–11]

Wilson's disease (WD) is an autosomal recessive disorder of copper metabolism that leads to the accumulation of copper in different tissues.[12] In neurological WD, the accumulation of copper and its resultant cytotoxicity affects the cortical and subcortical structures of the brain. However, WM abnormalities in WD are seldom studied.[13] The existing literature estimates WM involvement in 10–41% of patients with WD.[13] In a previous study, Van Wassenaer-van Hall *et al.*[13] observed WM of the dentato-rubral tract, thalamo-ponto-cerebellar fibers, and corticospinal tracts to be preferentially involved. If WD is left untreated, irreversible neuronal loss, degeneration, gliosis, and vacuolization may occur.[13–17]

The involvement of the CC in WD is known.[15,18–22] A study by Trocello *et al.*[15] demonstrated signal changes in the selenium of CC. However, this result could not be confirmed in diffusion tensor imaging studies. Hence, segment-specific involvement of the CC in WD is still debated. It is a personal observation of the authors that the CC appeared thinned out in many patients of WD, despite adequate chelation and absence of CC signal changes. The loss of area of the CC may have significant repercussions since it believed to be associated with cognitive dysfunction. It is well known that patients with WD may have poor scholastic performance and cognitive disturbances, irrespective of their treatment status.[17,23] It is hence possible that CC may be involved in WD and may be linked to cognitive dysfunction.

In this study, we attempted to identify the morphometric changes of CC by studying its macrostructural properties. Due to its well-defined boundaries and the easily discernible macroscopic properties, the morphometric parameters of the midsagittal CC can be easily

Europe PMC Funders Author Manuscripts

studied without using complex structural analytical techniques such as tractography or tract-based spatial statistics.[24] Furthermore, the topographic arrangement of fibers in CC provides a window to discern the cortical involvement due to the direct correlation of cross-sectional area with the fiber count of the cortical projections.[24,25] The projection fibers converge into a contiguous mass at the midsagittal plane and then diverge outwards to the cerebral cortex. We used a previously used and validated automated thickness profiling pipeline to measure the cross-sectional area and thickness profile of the CC segments.[24,25] The clinical, cognitive, and biochemical correlates of segmental involvement of CC were also assessed.

Methods

This study is a retrospective study performed at the Department of Neurology and the Department of Neuroimaging and Interventional Radiology at a tertiary care center. The clinical data and archived magnetic resonance imaging (MRI) scans of 14 patients with WD undergoing treatment were retrieved and analyzed. Ethical approval was waived-off by the Ethics Committee due to the retrospective nature of the study.

Clinical data

The clinical details of patients such as age, age at onset of neurological symptoms, duration of disease, MMSE score, and biochemical parameters such as serum copper, serum-free copper, 24 h urine copper, and ceruloplasmin levels at the time of MRI were obtained from case records. The age at onset was regarded as the age at which the first neurological symptom was experienced by the patient. The duration of disease was calculated based on the number of years from the onset of the first neurological symptom until the MRI acquisition.

MRI data

MRI scans of 14 patients with WD were retrieved from the database. All MRI scans were performed in a 3-T Philips Achieva MRI scanner with a 32-channel SENSE head coil. Sequences were obtained using the following parameters: high-resolution 3D T1-weighted anatomical images of 1 mm slice thickness, TR/TE = 8.1/3.7 ms; FOV = 256 × 256 × 115; sense factor = 3.5; flip angle = 8°; voxel size = 1 × 1 × 1 mm; acquisition matrix = 256 × 256, and a total of 165 sagittal slices without any inter-slice gap was used for the study. Furthermore, MRI scans of 14 age- and gender-matched subjects with no known comorbidities from the Indian population were selected as healthy controls for the final analysis.

CC morphology

The thickness and cross-sectional area were assessed using an automated pipeline.[21,22] Using a combination of the FSL-FLIRT registration tools and acpcdetect, the mid-sagittal plane was identified.[26,27] Subsequently, all MRI datasets were aligned and automated segmentation of the CC was performed. The data were further refined using mathematical morphological operations and post-processing steps to remove the posterior and pericallosal vessels. Thickness and surface area profiles in the form of non-overlapping contour lengths

were generated [Figure 1].[24,28] The CC was divided into five sections viz., anterior, mid-anterior, central, mid-posterior, and posterior CC segments, based on the Hofer–Frahm parcellation scheme based on DTI data.[8] The theoretical aspects and step-by-step methods for area and thickness profiling is out of scope for this article and are available in the article by Adamson *et al*.[24,25] The normalized CC cross-sectional areas were compared between patients and healthy controls with *t*-test using age, gender, and total intracranial volume as covariates and Bonferroni correction. A statistical threshold of $P < 0.05$ after correction for multiple comparisons was considered significant.

Statistical analysis

The clinical and demographic data were compared between patients and controls using *t*-test with Bonferroni correction. Nominal variables were compared using χ^2 test. Pearson's correlation was performed between the cross-sectional area of CC segments and clinico-biochemical variables (age at onset, duration of disease, MMSE, serum copper, serum-free copper, 24 h urine copper, and ceruloplasmin levels). A threshold of $P < 0.05$ after correction for multiple comparisons was considered as statistically significant.

Results

This study included 14 patients with WD (male: female = 10: 4). The mean age at the onset of symptoms was 15.3 ± 6.2 years, and the mean duration of disease at the time of MRI was 18.7 ± 9.7 months. The mean serum ceruloplasmin, serum copper, serum-free copper, 24 h urine concentration in patients was 6.17 ± 2.2 mg/dL (normal: 15–35 mg/dL), 46.84 ± 41.0 μg/dL (normal: 70–150 μg/dL), 18.2 ± 16.7 μg/dL (normal: 8–12 μg/dL), and 462 ± 234.6 μg/24 h (20–50 μg/24 h), respectively. The mean MMSE score was 21.9 ± 4.6. The clinical features in the cohort included the presence of Kayser–Fleischer ring (100%), parkinsonism (78.5%), dysarthria (78.5%), dystonia (71.4%), cognitive impairment (71.4%), behavioral disturbance (64.2%), pyramidal signs (64.2%), and tremor (57.1%) [Table 1]. Six patients were already on chelation therapy at the time of MRI [Table 1]. Ten patients had signal changes in the cortical or subcortical structures. However, none of the subjects had signal changes of the CC.

A significant difference in the mean area was observed only in CC_2 (WD vs. HC: 94.2 ± 25.5 vs. 118.6 ± 19.7 mm^2, corrected $P < 0.05$). Midsagittal areas of CC_1, CC_3, CC_4, and CC_5 segments were not significantly different in patients and controls [Table 2]. Significant difference in the mean thickness was observed in CC_1 (WD vs. HC: 5.06 ± 1.15 vs. 6.93 ± 0.89 mm, corrected $P < 0.05$), CC_2 (WD vs. HC: 3.73 ± 0.96 vs. 4.87 ± 1.01 mm, corrected $P < 0.05$), and CC_3 segments (WD vs. HC: 3.42 ± 0.84 vs. 3.94 ± 0.72 mm, corrected $P < 0.05$) [Table 2 and Figure 2].

A significant inverse correlation was present between earlier age at onset and decreasing mid-sagittal area of CC_2 ($R^2 = 0.53$, corrected $P < 0.05$) and CC_3 segments ($R^2 = 0.45$, corrected $P < 0.05$). A significant inverse correlation was present between earlier age at onset and decreasing thickness of CC_1 ($R^2 = 0.67$, corrected $P < 0.05$) and CC_2 segments ($R^2 = 0.53$, corrected $P < 0.05$). A mild but significant positive correlation was present between higher MMSE and increasing thickness of CC_1 ($R^2 = 0.38$, corrected $P < 0.05$) and

CC_2 segments (R^2= 0.24, corrected $P < 0.05$). There was no significant correlation between other clinical and biochemical variables (duration of disease, serum copper, serum-free copper, 24 h urinary copper, and ceruloplasmin levels) with cross-sectional area or thickness of any CC segments [Supplementary Table 1].

Discussion

Our findings confirm that the CC is discretely involved in WD and predominantly affects the anterior, mid-anterior, and middle segments of the CC. In this study, we obtained significant loss of cross-sectional area of CC_2 segment and loss of thickness of CC_{1-3} segments. Furthermore, earlier age at onset of neurological symptoms was associated with loss of area of CC_2 and CC_3 segments and thickness of CC_1 and CC_2 segments. MMSE score was significantly associated with loss of thickness of CC_1 and CC_2 segments. The duration of disease and biochemical variables were not significantly associated with loss of area or thickness of any CC segment.

The decrease in the surface area and thickness of the CC compared with healthy controls signifies the presence of WM loss, which in turn represents a decrease in the homotopic or heterotopic projections to the contralateral hemisphere.[8] Topographically, the CC_1 segment consists of projection fibers connecting the prefrontal lobe; the CC_2 segment consists of projection fibers connecting the premotor (PM) and supplementary motor cortical areas (SMA), and the CC3 segment consists of fibers connecting the motor cortex (M1) of both sides.[8] The loss of these axonal projections may have significant clinical implications in WD. It is now well known that frontal lobe involvement can cause cognitive deficits.[1,29,30] Furthermore, the PM, SMA, and M1 are key players in the frontal-subcortical loop of the motor circuitry and is implicated in the genesis of postural tremor in WD.[30] Hence, the cognitive and motor symptoms in our cohort may be partially explained by the involvement of anterior, mid-anterior, and middle segments of the CC.

Another important observation from our study was that the decrease in area of CC_2 and CC_3 and thickness of CC_1 and CC_2 segments were found to have a significant correlation with the age at onset of neurological symptoms. This implies that patients with an earlier onset of neurological manifestations have greater loss of CC fibers. Although the pathological processes of copper-induced cytotoxicity start very early, the neurological manifestations of WD usually appear only in the second decade of life.[12] An earlier onset of neurological signs probably implies a greater dysfunction in handling of the copper load, resulting in cytotoxicity and neuronal loss. Recently, genetic factors such as polymorphisms of *ApoE*, prion-related proteins, and *Mthfr* genes were reported to influence the age at onset and severity of symptoms.[12,31] Although the status of these polymorphisms in our cohort is unknown, it is possible that in the early disease state, neuronal loss may be more severe causing irreversible involvement of the CC. Hence, early screening of vulnerable population should be performed to prevent permanent sequelae.

This study also identified a significant correlation of MMSE score with the thickness of CC_1 and CC_2 segments. This is of interest since the CC coordinates different cognitive functions and interhemispheric connectivity.[31–33] Tractography studies have revealed significant

connectivity of anterior callosal regions with the frontal cortical areas and brain-behavioral links to cognitive and motor functions.[8,34] This suggest that the loss of CC fibers of the anterior segment is linked to the loss of neurons in the frontal cortex. There is converging evidence from neuropsychological and imaging studies which also supports the involvement of the frontal lobe in WD. It is now well established that the neuropsychological deficits in WD are predominantly frontal dysexecutive dysfunction.[29,34,35] Neuroimaging studies have also confirmed the presence of frontal and temporal atrophy in WD.[34,35] Hence, the association of MMSE score with the thickness of anterior and mid-anterior CC is biologically plausible. A similar association of cognitive function with CC loss is reported Parkinson's disease and Alzheimer's disease.[9–11]

The duration of disease, serum copper, serum-free copper, 24 hour urine copper, and ceruloplasmin levels did not correlate with the morphometric measures of any segment in this study, suggesting that there was no effect of these variables on CC morphometry. However, these results may be due to the smaller sample size and the heterogeneity of patients, especially with respect to treatment. Few of the patients were already on chelation for variable periods of time at the time of MRI. This may have altered the disease severity and copper profile of patients.

This study had few merits and limitations. First, we have demonstrated a segment-specific involvement of CC in WD. The observed abnormalities can account for the motor and cognitive dysfunction observed in our cohort. Secondly, the automated software pipeline used for this study is relatively easy to perform and is operator-independent, thereby removing any observer bias. The approach can also be performed on routine T1 sequences of MRI without any special sequences.

One of the major limitations of this study is the small sample size that limits its generalizability. Hence, validation of our findings may be required in a larger cohort of patients. Furthermore, this study used a heterogeneous cohort with respect to chelation therapy. This may have altered the course of the disease and involvement of brain structures. Assessing the cortical thickness in our cohort would have provided key information on the nature of cortical and CC involvement in WD. However, this could not be performed since many of our subjects had signal changes in the cortical and subcortical structures which could cause segmentation errors. Hence, the question of whether CC involvement is primarily due to cytotoxicity affecting WM fibers or is secondary to cortical involvement cannot be clarified. Due to the limited sample size, it was also not possible to re-stratify patients based on chelation status, gender, age, or biochemical values. Although widely used in clinical practice, the MMSE or its pediatric counterpart are not very robust measure of cognitive impairment. A detailed neuropsychological assessment with tests appropriate for children and young adults would have provided a better understanding of the cognitive dysfunction in WD. Additionally, the size of the CC is known to be dependent on various factors such as age, gender, ethnicity, socioeconomic status, race, and genetics. Hence, the influence of other possible confounders in our cohort cannot be ruled out. Lastly, the use of automated analysis also requires understanding of the associated software and also runs the risk of segmentation errors. Future studies in larger and more homogeneous cohorts should be performed to understand the differential impact of WD on CC. A sufficiently powered

study could also provide normative data for normal and abnormal CC area and thickness in different segments, making it more applicable in clinical settings.

Supplementary Material

Refer to Web version on PubMed Central for supplementary material.

Financial support and sponsorship

Nil.

References

1. Huang H, Zhang J, Jiang H, Wakana S, Poetscher L, Miller MI, et al. DTI tractography based parcellation of white matter: Application to the mid-sagittal morphology of corpus callosum. Neuroimage. 2005; 26: 195–205. [PubMed: 15862219]
2. Aboitiz F, Scheibel AB, Fisher RS, Zaidel E. Fiber composition of the human corpus callosum. Brain Res. 1992; 598: 143–53. [PubMed: 1486477]
3. Hasan KM, Kamali A, Kramer LA, Papnicolaou AC, Fletcher JM, Ewing-Cobbs L. Diffusion tensor quantification of the human midsagittal corpus callosum subdivisions across the lifespan. Brain Res. 2008; 1227: 52–67. [PubMed: 18598682]
4. Lebel C, Caverhill-Godkewitsch S, Beaulieu C. Age-related regional variations of the corpus callosum identified by diffusion tensor tractography. Neuroimage. 2010; 52: 20–31. [PubMed: 20362683]
5. Chao YP, Cho KH, Yeh CH, Chou KH, Chen JH, Lin CP. Probabilistic topography of human corpus callosum using cytoarchitectural parcellation and high angular resolution diffusion imaging tractography. Hum Brain Mapp. 2009; 30: 3172–87. [PubMed: 19241418]
6. Luders E, Thompson PM, Toga AW. The development of the corpus callosum in the healthy human brain. J Neurosci. 2010; 30: 10985–90. [PubMed: 20720105]
7. Witelson SF. Hand and sex differences in the isthmus and genu of the human corpus callosum. A postmortem morphological study. Brain. 1989; 112 (Pt 3) 799–835. [PubMed: 2731030]
8. Hofer S, Frahm J. Topography of the human corpus callosum revisited—Comprehensive fiber tractography using diffusion tensor magnetic resonance imaging. Neuroimage. 2006; 32: 989–94. [PubMed: 16854598]
9. Prendergast DM, Karlsgodt KH, Fales CL, Ardekani BA, Szeszko PR. Corpus callosum shape and morphology in youth across the psychosis spectrum. Schizophr Res. 2018; 199: 266–73. [PubMed: 29656909]
10. Goldman JG, Bledsoe IO, Merkitch D, Dinh V, Bernard B, Stebbins GT. Corpus callosal atrophy and associations with cognitive impairment in Parkinson disease. Neurology. 2017; 88: 1265–72. [PubMed: 28235816]
11. Wiltshire K, Camicioli R, Kaye JA, Small BJ. Corpus callosum in neurodegenerative diseases: Findings in Parkinson's disease. Dement Geriatr Cogn Disord. 2005; 7: 345–51.
12. Bruha R, Marecek Z, Pospisilova L, Nevsimalova S, Vitek L, Martasek P, et al. Long-term follow-up of Wilson disease: Natural history, treatment, mutations analysis and phenotypic correlation. Liver Int. 2011; 31: 83–91. [PubMed: 20958917]
13. van Wassenaer-van Hall HN, van den Heuvel AG, Jansen GH, Hoogenraad TU, Mali WP. Cranial MR in Wilson disease: Abnormal white matter in extrapyramidal and pyramidal tracts. AJNR Am J Neuroradiol. 1995; 16: 2021–7. [PubMed: 8585490]
14. Trocello JM, Broussolle E, Girardot-Tinant N, Pelosse M, Lachaux A, Lloyd C, et al. Wilson's disease, 100 years later…. Rev Neurol (Paris). 2013; 169: 936–43. [PubMed: 24119853]
15. Trocello JM, Guichard JP, Leyendecker A, Pernon M, Chaine P, El Balkhi S, et al. Corpus callosum abnormalities in Wilson's disease. J Neurol Neurosurg Psychiatry. 2011; 82: 1119–21. [PubMed: 20660913]

16. Kim TJ, Kim IO, Kim WS, Cheon JE, Moon SG, Kwon JW, et al. MR imaging of the brain in Wilson disease of childhood: Findings before and after treatment with clinical correlation. AJNR Am J Neuroradiol. 2006; 27: 1373–8. [PubMed: 16775300]

17. Beinhardt S, Leiss W, Stättermayer AF, Graziadei I, Zoller H, Stauber R, et al. Long-term outcomes of patients with Wilson disease in a large Austrian cohort. Clin Gastroenterol Hepatol. 2014; 12: 683–9. [PubMed: 24076416]

18. Sinha S, Taly AB, Ravishankar S, Prashanth LK, Venugopal KS, Arunodaya GR, et al. Wilson's disease: Cranial MRI observations and clinical correlation. Neuroradiology. 2006; 48: 613–21. [PubMed: 16752136]

19. Prashanth LK, Sinha S, Taly AB, Vasudev MK. Do MRI features distinguish Wilson's disease from other early onset extrapyramidal disorders? An analysis of 100 cases. Mov Disord. 2010; 25: 672–8. [PubMed: 20437536]

20. Sinha S, Taly AB, Prashanth LK, Ravishankar S, Arunodaya GR, Vasudev MK. Sequential MRI changes in Wilson's disease with de-coppering therapy: A study of 50 patients. Br J Radiol. 2007; 80: 744–9. [PubMed: 17709362]

21. Lawrence A, Saini J, Sinha S, Rao S, Naggappa M, Bindu PS, et al. Improvement of diffusion tensor imaging (DTI) parameters with decoppering treatment in Wilson's disease. JIMD Rep. 2016; 25: 31–7. [PubMed: 26122629]

22. Dong T, Yang W-M, Wu M-C, Zhang J, Huang P, Xu C-S, et al. Microstructure changes in whiter matter relate to cognitive impairment in Wilson's disease. Biosci Rep. 2019; 15: 39.

23. Walshe JM. The conquest of Wilson's disease. Brain. 2009; 132: 2289–95. [PubMed: 19596747]

24. Adamson CL, Wood AG, Chen J, Barton S, Reutens DC, Pantelis C, et al. Thickness profile generation for the corpus callosum using Laplace's equation. Hum Brain Mapp. 2011; 32: 2131–40. [PubMed: 21305661]

25. Adamson C, Beare R, Walterfang M, Seal M. Software pipeline for midsagittal corpus callosum thickness profile processing: Automated segmentation, manual editor, thickness profile generator, group-wise statistical comparison and results display. Neuroinformatics. 2014; 12: 595–614. [PubMed: 24968872]

26. Stezin A, George L, Jhunjhunwala K, Lenka A, Saini J, Netravathi M, et al. Exploring cortical atrophy and its clinical and biochemical correlates in Wilson's disease using voxel based morphometry. Parkinsonism Relat Disord. 2016; 30: 52–7. [PubMed: 27372240]

27. Ardekani BA, Bachman AH. Model-based automatic detection of the anterior and posterior commissures on MRI scans. Neuroimage. 2009; 46: 677–82. [PubMed: 19264138]

28. Jenkinson M, Smith S. A global optimisation method for robust affine registration of brain images. Med Image Anal. 2001; 5: 143–56. [PubMed: 11516708]

29. Gutiérrez-Ávila N, Zúñiga-Márquez J, Burgos-Torres N, Arias-Valencia J, Quintero-Cusguen P, Acosta-Barreto R. Dysexecutive syndrome in a patient with Wilson's disease. Psychology. 2014; 05: 47–52.

30. Südmeyer M, Pollok B, Hefter H, Gross J, Butz M, Wojtecki L, et al. Synchronized brain network underlying postural tremor in Wilson's disease. Mov Disord. 2006; 21: 1935–40. [PubMed: 16991150]

31. Chen C, Shen B, Xiao JJ, Wu R, Duff Canning SJ, Wang XP. Currently clinical views on genetics of Wilson's disease. Chin Med J (Engl). 2015; 128: 1826–30. [PubMed: 26112727]

32. Doron KW, Gazzaniga MS. Neuroimaging techniques offer new perspectives on callosal transfer and interhemispheric communication. Cortex. 2008; 44: 1023–9. [PubMed: 18672233]

33. Jarbo K, Verstynen T, Schneider W. In vivo quantification of global connectivity in the human corpus callosum. Neuroimage. 2012; 59: 1988–96. [PubMed: 21985906]

34. Wenisch E, De Tassigny A, Trocello JM, Beretti J, Girardot-Tinant N, Woimant F. Cognitive profile in Wilson's disease: A case series of 31 patients. Rev Neurol (Paris). 2013; 169: 944–9. [PubMed: 24120329]

35. Hegde S, Sinha S, Rao SL, Taly AB, Vasudev MK. Cognitive profile and structural findings in Wilson's disease: A neuropsychological and MRI-based study. Neurol India. 2010; 58: 708–13. [PubMed: 21045492]

Europe PMC Funders Author Manuscripts

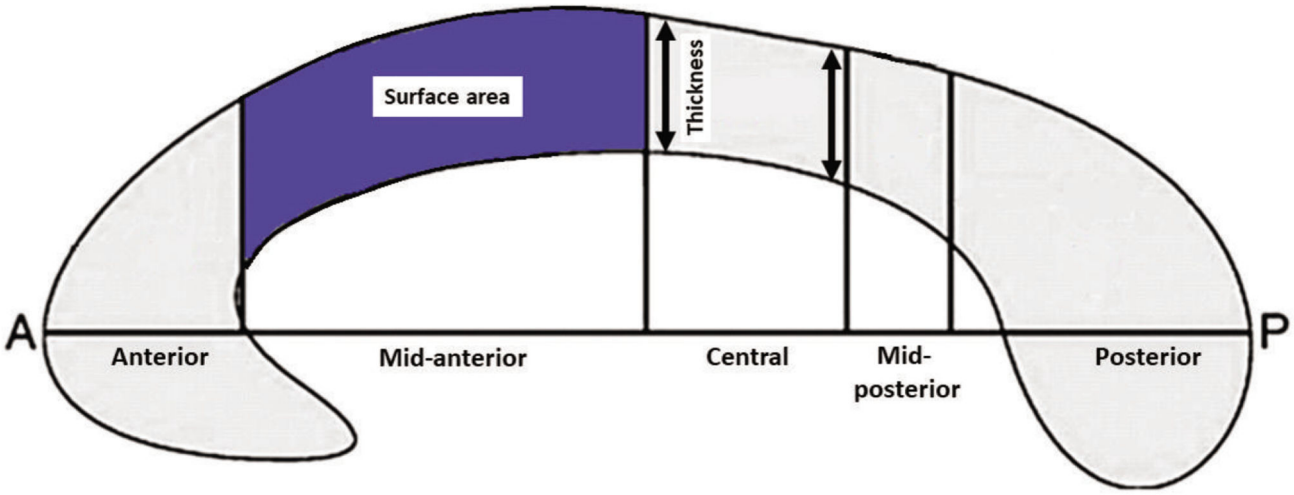

Figure 1. Figurative representation of the area and thickness measures of the CC

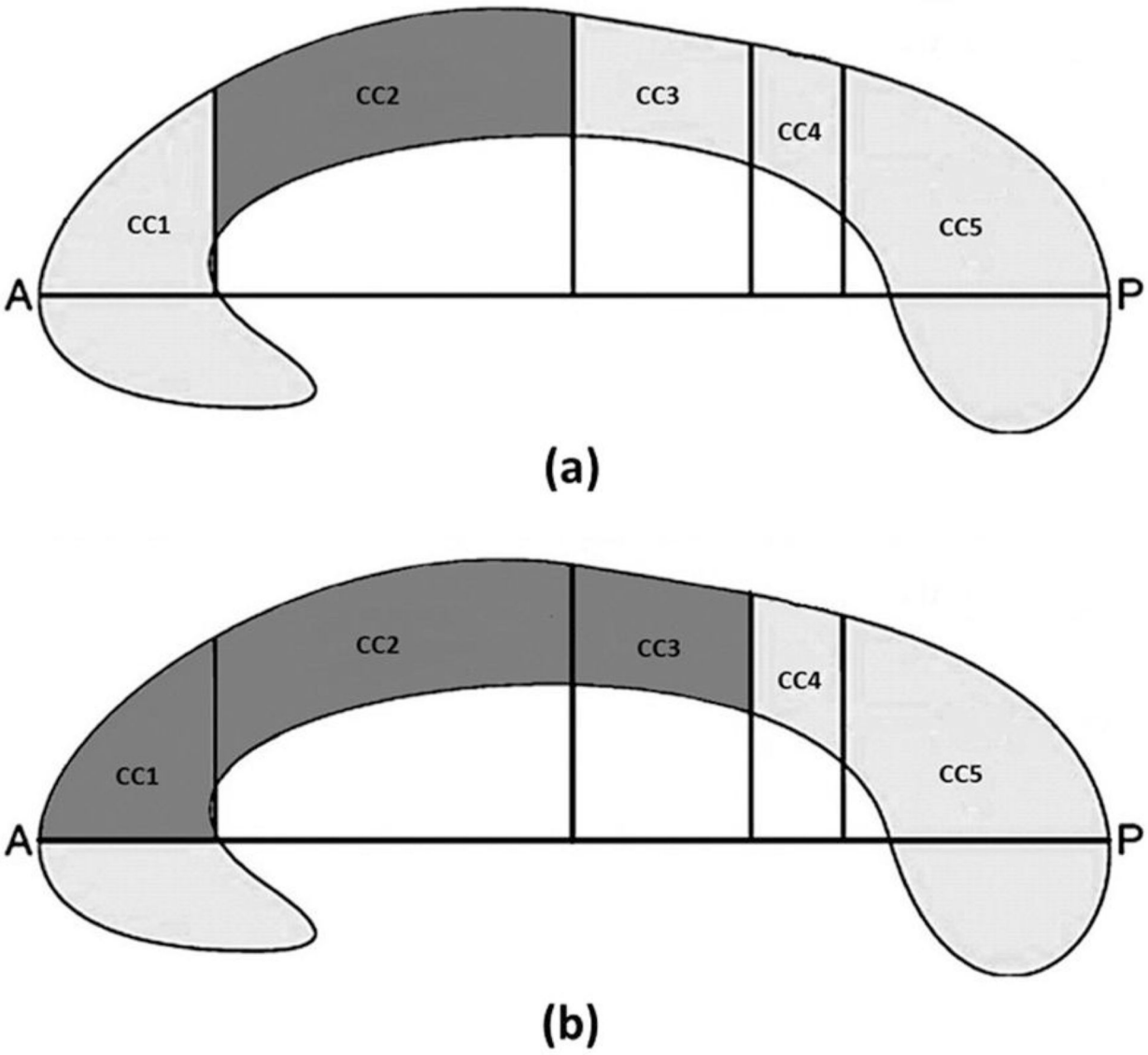

Figure 2. CC segments with significant differences in morphological profiles.

(A) Mean cross-sectional area was significantly different in CC_2 segment (corrected *p*-value <0.05). (B) Mean thickness was significantly different only in CC_1, CC_2, and CC_3 segments (corrected *p*-value <0.05)

Table 1

Clinical details of patients with WD

Characteristics	Wilson's disease (*n* = 14)	Healthy controls (*n* = 14)
Age (in years)	17.1 ± 76	16.8 ± 5.9
Gender distribution (male: female)	10:4	10:4
Age at onset of neurological symptoms (in years)	15.3 ± 6.2	—
Duration of disease at MRI (in months)	18.7 ± 9.7	—
Drug naive	8 (57%)	—
Mean MMSE score	21.9 ± 4.6	28.6 ± 1.2
Serum copper (in μg/dL)	46.84 ± 41.0	—
Serum ceruloplasmin (in mg/dL)	6.17 ± 2.20	—
Serum-free copper (in μg/dL)	18.2 ± 16.7	—
24 h urine copper concentration (in μg/24 h)	462 ± 234.6	—
Clinical features		
Kayser–Fleischer ring	14 (100%)	-
Parkinsonism	11 (78.5%)	-
Dysarthria	11 (78.5%)	-
Dystonia	10 (71.4%)	-
Cognitive impairment	10 (71.4%)	-
Behavioral disturbance	9 (64.2%)	-
Pyramidal signs	9 (64.2%)	-
Tremor	8 (57.1%)	-
Chorea	5 (35.7%)	-
Dysphagia	4 (28.5%)	-
Cerebellar signs	3 (21.4%)	-
Seizures	3 (21.4%)	-

Data expressed as mean ± standard deviation or number (percentage). Normal reference range: serum ceruloplasmin: 15–35 mg/dL, serum copper: 70–150 μg/dL, serum-free copper: 8–12 μg/dL, 24 h urine copper concentration: 20–50 μg/24 h

Europe PMC Funders Author Manuscripts

Table 2

Morphological profile of CC segments in patients with WD and healthy controls

Mean area of CC segment (mm2)				Mean thickness of CC segment (mm)		
CC	**WD**	**HC**	***p* -value**	**WD**	**HC**	***p*-value**
CC_1	61.63 ± 10.25	62.77 ± 10.24	N.S.	5.06 ± 1.15	6.93 ± 0.89	<0.05
CC_2	94.22 ± 25.52	118.66 ± 19.78	<0.05	3.73 ± 0.96	4.87 ± 1.01	<0.05
CC_3	41.15 ± 9.59	47.48 ± 7.73	N.S.	3.42 ± 0.84	3.94 ± 0.72	<0.05
CC_4	20.68 ± 4.46	22.70 ± 5.31	N.S.	3.30 ± 0.99	3.63 ± 0.88	N.S.
CC_5	117.52 ± 17.57	120.27 ± 18.55	N.S.	6.48 ± 1.64	6.77 ± 1.84	N.S.

N.S. = non-significant, WD = Wilson's disease, HC = healthy controls; CC = corpus callosum.
All *p*-values were corrected for multiple comparisons